International Journal of Fatigue 120 (2019) 162–174

Contents lists available at ScienceDirect

International Journal of Fatigue

journal homepage: www.elsevier.com/locate/ijfatigue

Evaluating the use of rate-based monitoring for improved fatigue remnant life predictions

Michael Siu Hey Leung[a,*], Joseph Corcoran[a], Peter Cawley[a], Michael D. Todd[b]

[a] Department of Mechanical Engineering, Imperial College London, UK
[b] Jacob School of Engineering, University of California San Diego, United States

ARTICLE INFO

Keywords:
Life prediction
Probabilistic analysis
Failure Forecast Method
Structural health monitoring

ABSTRACT

The ability to perform accurate remnant life predictions is crucial to ensure the integrity of engineering components that experience fatigue loading during operation. This is conventionally achieved with periodic inspections, where results from non-destructive evaluation and estimation of the operating conditions are obtained to perform remnant life predictions using empirical crack growth laws. However, remnant life predictions made with this approach are very sensitive to their input parameters; uncertainty in each parameter would aggregate and result in great uncertainty in the final prediction. With the increasing viability of permanently-installed systems, it is proposed that the *rate of damage growth* can be used to more accurately and confidently gauge the integrity of an engineering component and perform remnant life predictions using the Failure Forecast Method. A statistical analysis of an example fatigue crack growth test was performed to compare the uncertainties of the remnant life predictions made using the conventional inspection approach and the proposed rate-based monitoring approach. It is shown that the Failure Forecast Method produces significantly more accurate and confident predictions compared to the inspection approach. The use of the Failure Forecast Method under non-constant amplitude loading conditions was also investigated. An equivalent cycles method is introduced to accommodate step changes in operating conditions. The effect of load interactions was also studied through a fatigue test with isolated overloads and a random variable amplitude loading test. Overall, the study has shown that the frequent data obtained from permanently installed monitoring systems provides new opportunities in remnant life estimates and potentially opens the way to increasing the intervals between outages and safely reducing conservatism in life predictions.

1. Introduction

Fatigue damage is considered to be one of the leading causes of failure in a range of engineering applications. Under repeated loading, defects can initiate and propagate through engineering structures, resulting in catastrophic failure [1,2]. There are two main approaches to the evaluation of fatigue damage, namely the safe-life approach and the damage-tolerant approach. The safe-life approach considers the fatigue life of a nominally defect-free component, while the damage-tolerant approach considers the life of a component containing a defect [1]. The relevance of these approaches depends on multiple aspects of the specific engineering application. Some of these include the type of material, type of loading, consequence of failure and the cost of analysis. While the safe-life approach is more commonly used during the design of engineering components, the damage-tolerant approach remains relevant in particular for maintenance and life extension of components that have been in operation for some time and in which defects were detected from inspections. Understanding and monitoring fatigue crack growth therefore remains an active area of research for applications in multiple industries [3–5].

In applications where the damage-tolerant approach is used, periodic in-service non-destructive evaluation (NDE) inspections are traditionally conducted to identify any defects that have manifested during operation. Once a defect is found, a structural integrity assessment is performed to determine whether the defect would propagate under the operating conditions of the component, and if so, perform remnant life predictions using empirical crack growth laws. This would dictate whether the component is deemed safe to continue service or to necessitate repair or replacement.

Despite significant efforts in developing accurate models of fatigue crack growth, the predictions made by these models are very sensitive to uncertainties in input parameters, such as the measured defect

* Corresponding author.
E-mail address: michael.leung@ic.ac.uk (M.S.H. Leung).

https://doi.org/10.1016/j.ijfatigue.2018.11.012
Received 25 July 2018; Received in revised form 7 November 2018; Accepted 9 November 2018
Available online 14 November 2018
0142-1123/ © 2018 The Authors. Published by Elsevier Ltd. This is an open access article under the CC BY license (http://creativecommons.org/licenses/BY/4.0/).

geometry, material properties and loading conditions [6]. Consequently, and since fatigue damage accumulation is stochastic in nature [7], probabilistic approaches to fatigue life predictions have become increasingly popular. To ensure components can operate safely, very conservative estimates are made to ensure the probability of failure is below standardised levels [8,9].

With recent advances in technology, on-line structural health monitoring of engineering structures using permanently-installed monitoring systems become an increasingly viable solution to assess the structural health of engineering structures. Structural health monitoring can provide a continuous, real-time, estimate to how the actual component is responding to the actual operating conditions. Significant research is being conducted to develop technologies for structural health monitoring of engineering components susceptible to fatigue damage. Research has mainly focused on extensions to the conventional inspection approach of using empirical crack growth or damage accumulation laws where operating conditions and crack sizing data is provided by structural health monitoring systems rather than periodic inspection [10]. Examples include ways of monitoring the operating conditions of components [11], ways of detecting defect initiations such as vibration response monitoring [12] and acoustic emissions monitoring [13], or ways to monitor crack growth [14].

Despite the interest in fatigue damage, little research has been conducted into utilising the continuity of data that monitoring provides. One of the main benefits of using permanently installed sensors is that measurements may be taken much more frequently. This is illustrated in Fig. 1, which shows the results of a fatigue test; the crosses are analogous to data obtained via regular in-service inspections, while the dots represent data that can be obtained with monitoring. The frequent data collection enables accurate rate of change estimates and identification of trends in the data. It is proposed the rate of change information may be exploited for improved fatigue life predictions.

Fatigue damage is an example of a positive feedback mechanism [15]; an increase in damage leads to an increase in the rate of damage accumulation. Consequently, the fatigue crack growth rate behaviour has a characteristic form as can be seen in Fig. 1 [15]. This behaviour was first noted by Voight [16], who subsequently developed the Failure Forecast Method (FFM), which utilises this characteristic behaviour of positive feedback mechanisms to perform remnant life predictions. Compared to conventional damage assessment methods, the FFM does not rely on assumptions of material properties, geometry, or operating conditions, but rather the observed response of the component. This reduces the number of sources of uncertainty and potentially provides more confident life predictions.

This paper starts by detailing the methodology of the conventional inspection and proposed monitoring approach to perform fatigue life predictions. Example laboratory fatigue tests are used to generate example data sets which are used to compare the two approaches. A probabilistic analysis is used to quantify the uncertainty of the conventional inspection approach, while regression analysis is used to evaluate the predictions of the Failure Forecast Method; a comparison of the accuracy and confidence of the remnant life predictions then follows. Methods for utilising the Failure Forecast Method for remnant life prediction for non-constant amplitude loading are evaluated; step changes in loading, isolated overloads and pseudo-random amplitude loading are being covered. The paper concludes with discussion and conclusions on the applicability of rate-based monitoring for industrial applications.

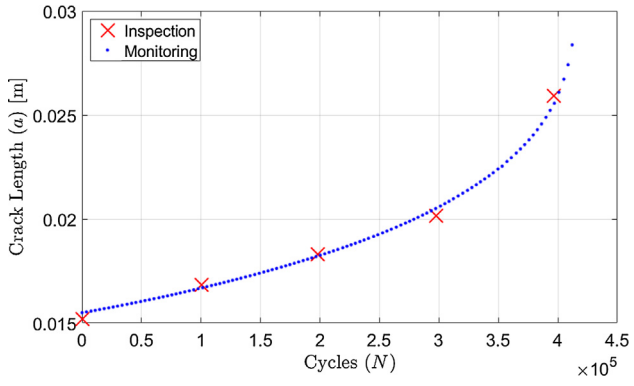


Fig. 1. Plot of crack length against number of loading cycles of a fatigue test. The crosses are analogous to data obtained via regular in-service inspections, while the dots represent the continuity of data obtainable by monitoring.

2. Inspection approach to remnant life predictions

2.1. Review of methodology

Using the conventional inspection approach, when defects are found with NDE inspections and sufficient information on the operating conditions, material properties and geometry of the component is available, empirical crack growth laws can be used to perform fatigue life predictions. There are many empirical crack growth laws available, the simplest being the Paris crack growth law [17], which is widely used to evaluate fatigue life calculations in engineering applications across different industries [18,8,9]. The Paris law is given as,

$$\frac{da}{dN} = C(\Delta K)^m = C(Y(a)\Delta\sigma\sqrt{a})^m \tag{1}$$

where C and m are material constants known as the Paris' constant and exponent respectively; ΔK is the stress intensity range as a result of stress range, $\Delta\sigma$, and crack length, a; $Y(a)$ is the geometry function as a function of crack length. Integrating from the initial crack length, a_0 to the failure crack length, a_f gives,

$$N_f = \int_{a_0}^{af} C^{-1}(Y(a)\Delta\sigma\sqrt{a})^{-m} da \tag{2}$$

where N_f is the remnant life prediction of the component.

As with many other modes of material failure, fatigue damage accumulation is by nature stochastic, hence probabilistic methodologies are needed to quantify uncertainties and determine the level of conservatism required [7,19]. A regularly-inspected component is deemed safe for continued operation if the probability of failure of the component is kept below a predefined threshold up to the next scheduled inspection. A reconstructed schematic of how inspections update the probability of failure from DNVGL-RP-C210 is shown in Fig. 2 [9]. If the probability of failure exceeds a critical value prior to the next scheduled inspection, its integrity would no longer be guaranteed, and actions will need to be taken to repair or replace the component. The critical probability of failure of the component is specific to each engineering application, mainly dictated by the risks and consequences involved should a failure occur. Therefore, confidence in life predictions is crucial to minimise conservatism and hence make it possible to safely operate the component closer to its actual failure time.

To demonstrate the inspection approach to performing fatigue life predictions, and to later compare with the proposed rate-based monitoring approach, a statistical analysis on a set of fatigue experimental data was conducted to establish the confidence of fatigue life predictions. The experiment uses a standard 316 stainless steel compact tension specimen; the geometry and loading parameters being given in Table 1 and Fig. 3. The crack propagation is monitored using a permanently-installed potential drop measurement system, but only one data point every 10^5 cycles are used to imitate the infrequent data available from inspections.

To evaluate the confidence in the life predictions, the uncertainties for all individual parameters will have to be quantified for the analysis as detailed in Table 2. A discussion on quantifying these values is given below. It is fully recognised that the assumptions made on the statistical variation of the input parameters are hugely simplistic; the

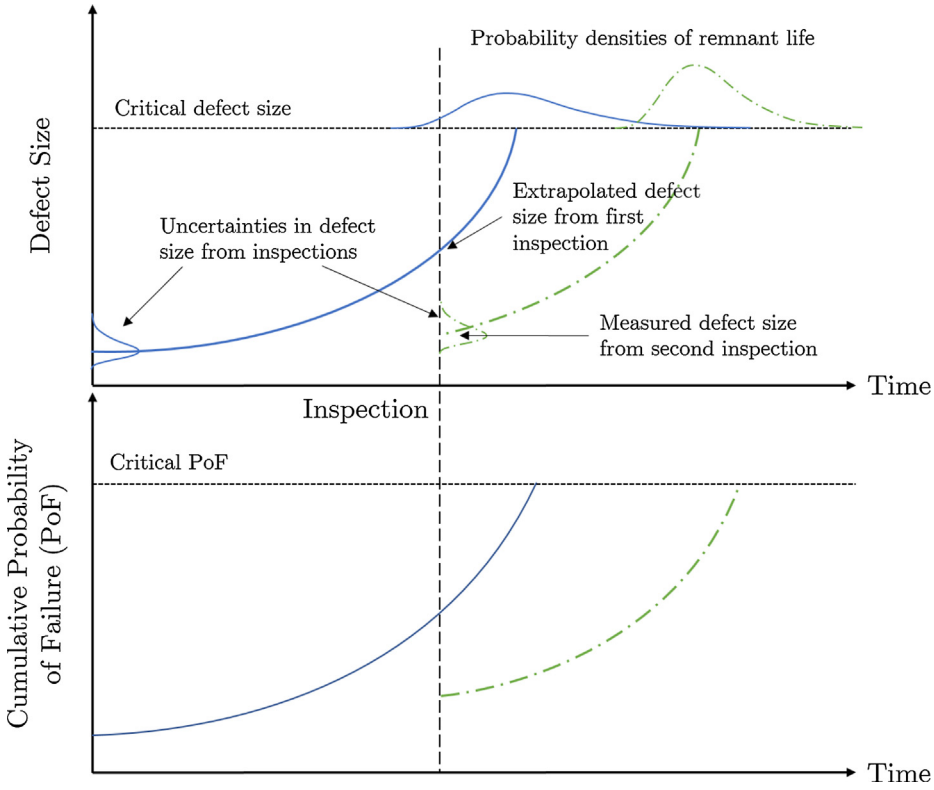


Fig. 2. Schematic reconstructed from the DNVGL Recommended Practice C210 showing how the probability of failure updates with an inspection [9].

Table 1
Geometry and loading parameters of the fatigue test in accordance to ASTM 647 [20] shown in Fig. 3.

Parameter	Value
W (mm)	50
B (mm)	25
a (mm)	15.5
Maximum load, P_{max} (kN)	11
Load ratio, R	0.1

Table 2
Table showing the quantified uncertainties for each input parameter of the empirical crack growth law used in the statistical analysis.

Parameter	Mean value	Standard error
Measured crack length, a_0 (mm)	Updates with each inspection	1
Critical crack length, a_f (mm)	38	Not considered
Paris constant, $ln(C)$	− 25.5	0.264
Paris exponent, m	2.88	Not considered
Maximum load, P_{max} (kN)	35	3.5
Load ratio, R	0.1	Not considered
Geometry, $Y(a)$	Calculated from standards	Not considered

uncertainties of the parameters are assumed to be independent, and the effect of uncertainty in geometry is not considered. However, it is believed that these assumptions are sufficient to illustrate how uncertainties of each input parameter aggregate to result in the overall

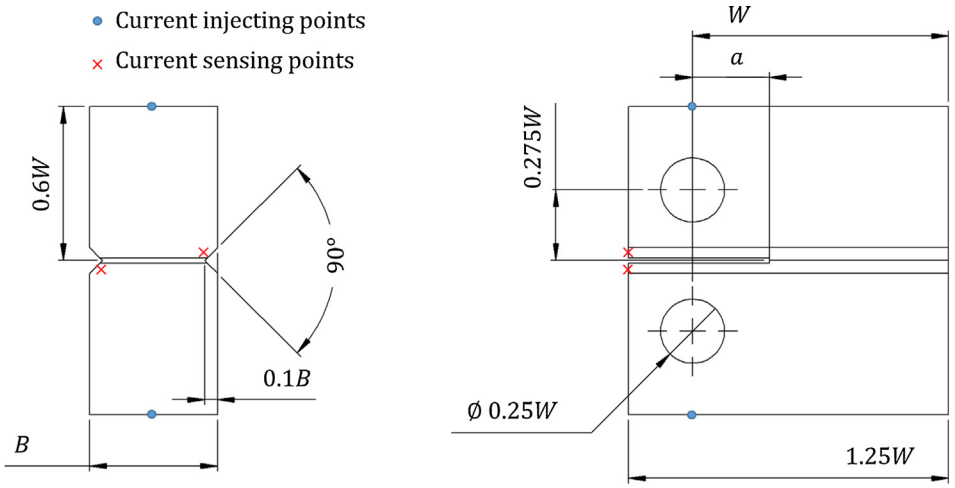


Fig. 3. Schematic showing the geometry of the specimen used in the experiment.

uncertainties in life predictions. The assumptions made here are optimistic and greater uncertainties are to be expected in industrial applications. This method offers a framework that may be used for the analysis of more specific examples.

Since crack growth in only one direction is considered in this analysis, the geometry of the defect can be characterised by a single crack length measurement, a_0. This measurement is updated every time an inspection is conducted. The error in defect size measured from NDE is assumed to be normally distributed with a standard deviation of 1 mm and no bias. This greatly depends on the NDE technique used as well as positioning and geometry of the defect. Other than the capabilities of the NDE technique, there are also other sources of uncertainties, such as the placement of measurement probes as well as calibration error [21]. The assumption made here is optimistic and is approximated with the nominal capabilities of a state-of-the-art NDE system [22].

The critical crack length a_f is often conservatively estimated from the plane strain fracture toughness of the component using linear elastic fracture mechanics. The uncertainty in this is not considered for the analysis as the final crack length has a relatively small effect on the final estimated failure cycle.

The Paris constant C and exponent m of a specific component are very rarely known with accuracy as they can vary even with the same material under nominally identical conditions as demonstrated by Virkler [6]. The constants are typically fitted retrospectively to fatigue test data to capture the stochastic nature and material variability, and hence exact values are unavailable when making life predictions. Standardised values and standard deviations of the Paris' constants from the British Standards 7910 [8] as shown in Table 2 are therefore used to simulate how analyses are typically done in industrial applications.

Lastly, the operating conditions of the component include loading cycles experienced, temperature of the environment and the effect of aggressive environments, all of which could have an effect on the crack growth characteristics. Only the nominal stress range $\Delta\sigma$ is considered in this analysis. The error in loading is assumed to be normally distributed with a standard error of 3.5 kN (10% of the maximum load) and no bias. The error in load ratio, R, is not considered. Again, an optimistic assumption is made here as the uncertainty in loading is highly dependent on the application and whether design load or loading data based on structural health monitoring is used.

2.2. Statistical analysis on remnant life predictions

Incorporating all these uncertainties, a 10,000-trial Monte-Carlo simulation was performed to evaluate the probability density function (PDF) of the remnant life of the component described earlier. All the input parameters are sampled randomly from their statistical distributions defined in Table 2 and kept constant for each trial, and the predicted N_f is calculated using Eq. (2). A log-normal distribution was then fitted to the simulation results to obtain statistical properties of the prediction [6].

The PDF of the predicted N_f prior to the experiment ($N = 0$, where N is the number of loading cycles the component has experienced) is plotted in Fig. 4. The point at which failure occurred during the experiment is shown with a dotted black line, which is at $N = 4.24 \times 10^5$. From the results of the analysis the confidence in the predicting remnant life can be quantified. The 3σ lower and upper confidence bounds at the beginning of the experiment were 2.10×10^5 and 2.26×10^6 respectively, showing that the confidence in the predicted N_f is rather low, with a 3σ confidence interval that spans over an order of magnitude. As previously discussed, it is necessary to adopt the lower bound estimate as the final prediction to ensure safe operation; large uncertainty therefore requires extreme conservatism.

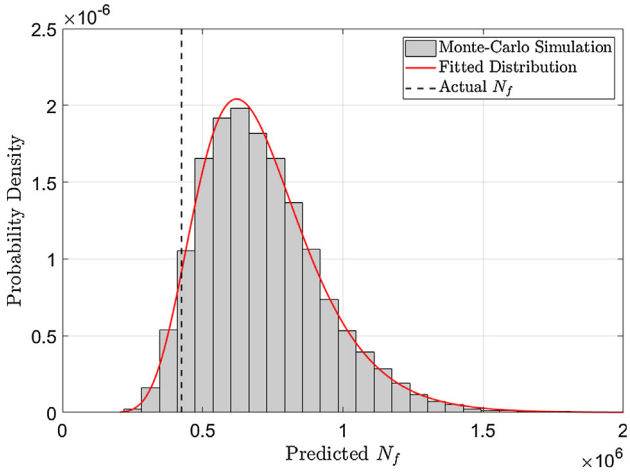


Fig. 4. Results of the Monte-Carlo simulation used to obtain the probability density function of the failure cycle at $N = 0$. The solid line shows the fitted log-normal distribution, and the dash line indicates the actual failure time of the experiment, $N_f = 4.24 \times 10^5$.

2.3. Inspection updating

With each inspection where a new crack length is obtained, the estimates of the variables $\Delta\sigma$ and C can also be updated using Bayesian updating. Bayes' theorem states that,

$$P\left(A\middle|B\right) = \frac{P(A) \times P(B|A)}{P(B)} \tag{3}$$

where $P(A)$ is the prior distribution, $P(B|A)$ is the likelihood, $P(B)$ is the marginal likelihood and $P(A|B)$ is the posterior distribution. Putting this in the context of an inspection of a fatigue crack, A is our estimate of the variables $\Delta\sigma$ and C, and B is the event of an inspection result. The likelihood function is obtained numerically by considering the probability of the resulting measurement given each combination of $\Delta\sigma$ and C. The marginal likelihood is simply the numerical integral of the likelihood function. Together with the prior knowledge on the distribution of the variables as detailed in Table 2, an updated estimate of the distribution of the variables can be obtained using Bayes' theorem. This process is done recursively with each inspection as the posterior distribution from the inspection becomes the prior distribution during the analysis of the next inspection.

The probability of failure after each new inspection is shown in Fig. 5, assuming that an inspection was performed every 10^5 cycles. As seen from the results in this particular case, the inspection-based approach is initially overestimating N_f, gradually converging to the actual N_f with each inspection being closer to failure. Further discussion is

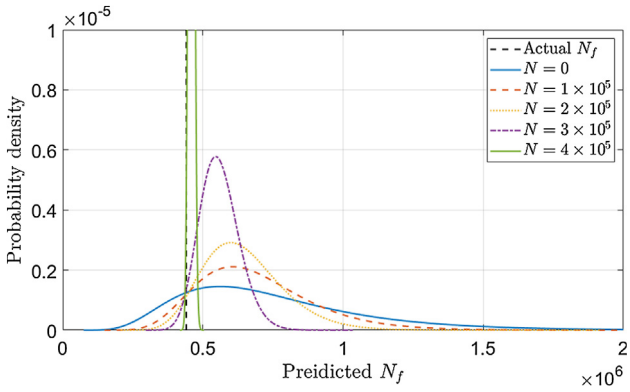


Fig. 5. Fitted log-normal distribution of the predicted failure cycle at every inspection made at intervals of 10^5 cycles.

given in Section 3.3, where the inspection approach is compared with the monitoring approach.

3. Monitoring approach to remnant life predictions

An alternative way of performing remnant life predictions is the monitoring approach. Instead of conducting periodic in-service inspections, a permanently-installed monitoring system can be installed to monitor the rate at which the damage accumulates. Remnant life predictions can then be performed in real-time while the component is in operation using the Failure Forecast Method (FFM).

3.1. Review of methodology

Voight first observed that the relationship,

$$\left(\frac{d\Omega}{dt}\right)^{-\alpha}\left(\frac{d^2\Omega}{dt^2}\right) - A = 0 \tag{4}$$

can be used to describe rate-dependent material failures such as fatigue crack growth, where Ω is an observable metric of damage and α and A are arbitrary constants [23]. He proceeds to state that the equation can be integrated for $\alpha > 1$ to give,

$$\left(\frac{d\Omega}{dt}\right)^{1-\alpha} = A\left(\alpha - 1\right)\left(t_f - t\right) + \left(\frac{d\Omega}{dt}\bigg|_f\right)^{1-\alpha} \tag{5}$$

where t_f is the failure time and $\frac{d\Omega}{dt}\Big|_{f'}$ is the rate of damage accumulation at failure.

The rate of damage accumulation at failure is often orders of magnitude greater than accumulation rates early on in fatigue life. It is therefore reasonable to assume that the rate of damage accumulation at failure to be infinite. Also, it is observed that for many cases including fatigue crack growth, $\alpha \approx 2$. A more detailed discussion on this by Corcoran can be found in [15]. Hence, applying the above assumption and putting Eq. (5) in the context of fatigue crack growth as a function of loading cycles, N,

$$\left(\frac{d\Omega}{dN}\right)^{-1} = A\left(N_f - N\right) \tag{6}$$

so,

$$N_f = N + \frac{1}{A}\left(\frac{d\Omega}{dN}\right)^{-1} \tag{7}$$

where Ω now becomes a generic sensor output of a monitoring system that changes with crack growth. This highlights one of the benefits of the FFM, which is the flexibility that is afforded to the monitoring technique. As the absolute crack length is not interpreted directly, but rather the relative change in rate, generic sensor outputs which are symptomatic of damage may be used as a proxy. In the examples used in this paper, resistance measurements from a potential drop technique are used as a generic metric of crack growth. A more comprehensive discussion on the requirements of the measurement and monitoring system can be found in [15].

Using Eq. (6), the failure cycle, N_f, can be estimated by performing a regression analysis on the inverse damage accumulation rate, $\left(\frac{d\Omega}{dN}\right)^{-1}$ against the number of loading cycles, then extrapolating the regression fit and finding the x-axis intercept where crack growth rate is infinite as schematically demonstrated in Fig. 6. By assuming $\alpha = 2$ such that the regression becomes linear, the prediction made would be the negative ratio between the intercept and slope of the regression fit. This method of performing remnant life predictions is known as the Failure Forecast Method (FFM).

To demonstrate the use of the FFM for remnant life predictions, the experimental results were analysed using the method, simulating a permanently-installed monitoring system being installed on the defective component while it continues operation. The rate of change in signal, in this case the resistance measurement, R, from the potential drop measurement system, is calculated to perform the FFM analysis without converting to crack length measurements as with typical analysis of potential drop measurement results. This is obtained from the slope of the linear regression fit performed on every 5 resistance measurements. The inverse of the rate of change in resistance, $\frac{dR}{dN}^{-1}$, is then calculated and a linear regression analysis of the data is performed to obtain the predicted N_f. Fig. 7 plots the results in intervals of 10^5 cycles. In this analysis, most recent $100\frac{dR}{dN}$ data points (or all data points when there are less than 100 points at the beginning) were used as indicated on the plot by the two vertical solid lines. The dash line indicates the actual failure cycle. Predictions are made in real-time as the component is fatigued, with the plot of predicted N_f against number of fatigue cycles shown in Fig. 8; again, the dotted line is where actual failure occurred.

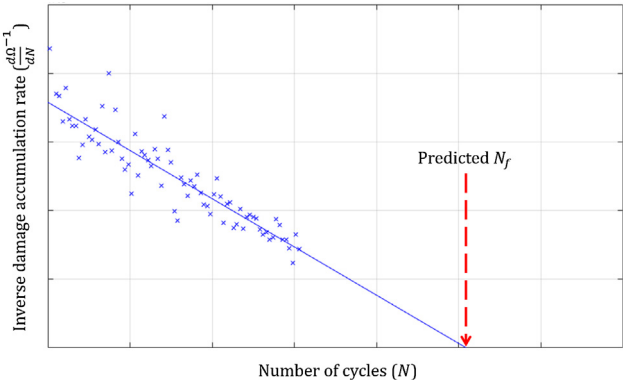


Fig. 6. Schematic illustration of the inverse damage accumulation rate $(\frac{d\Omega}{dN}^{-1})$ against number of cycles for a set of fatigue testing data to demonstrate the use of the FFM for remnant life predictions.

Utilising an on-line permanently-installed monitoring system that takes frequent measurements and hence provide continuous rate estimates, the predicted N_f can be continuously updated as more damage accumulation rate data is obtained in-service to provide real-time life predictions. The major advantage of using the FFM for life predictions is that minimal knowledge on the operating conditions is required. As opposed to predictions made with inspection results, parameters including loading conditions, material properties, geometry of the component and actual crack length measurements are not required. Assuming that all operating conditions remain constant, the only input required for the FFM is any input signal that can be used to measure the rate of damage accumulation.

3.2. Statistical analysis of remnant life predictions

As opposed to the inspection approach where empirical crack growth laws are used, the FFM simply uses the extrapolated point of infinite damage accumulation rate as the predicted failure time. Therefore, the only source of random uncertainty for the FFM is the random uncertainty in the damage accumulation rate measurements, which in turn results in uncertainties in the regression fit and the extrapolated x-axis intercept.

The distribution of the predicted failure cycle, $p(\hat{N}_f)$, can be analytically evaluated as demonstrated by Todd et al. [24]. The analytical solution is,

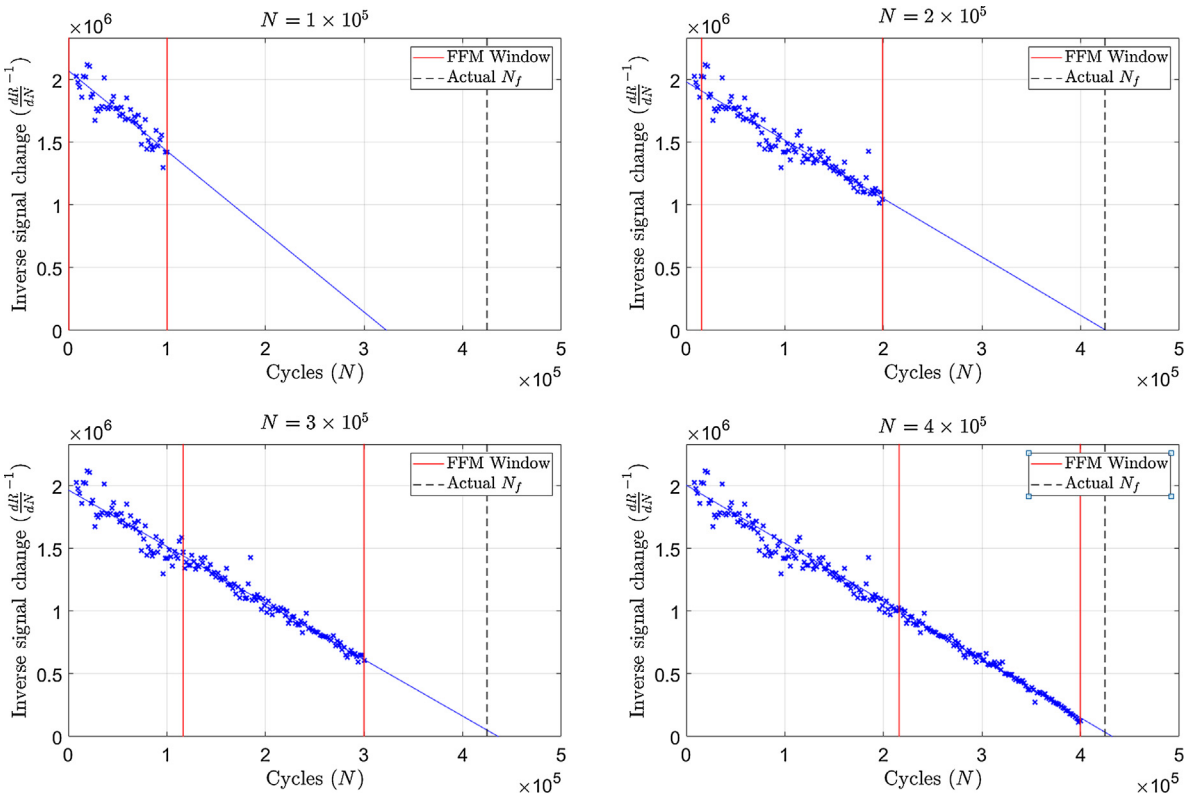


Fig. 7. Remnant life predictions made using the FFM at intervals of 10^5 cycles. The vertical solid lines indicate the window of $\frac{dR}{dN}$ data used for the FFM, and the dash line indicates the actual failure cycle.

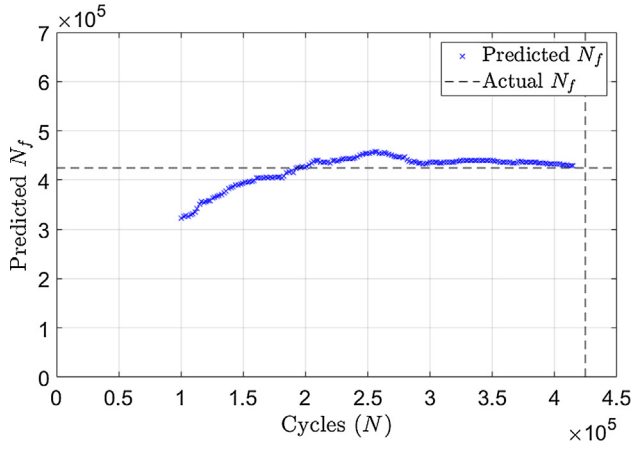


Fig. 8. Plot of predicted N_f against number of loading cycles for the fatigue experiment. Dash lines indicate the actual failure cycle.

$$p(\widehat{N}_f) = \frac{\sqrt{1-\rho^2}\,\sigma_0\sigma_1 e^{\frac{-\mu_1^2\sigma_0^2+2\rho\mu_0\mu_1\sigma_0\sigma_1-\mu_0^2\sigma_1^2}{2\sigma_0^2\sigma_1^2(1-\rho^2)}}}{\pi(\sigma_0^2+2\rho\sigma_0\sigma_1\widehat{N}_f+\sigma_1^2\widehat{N}_f^2)} e^{\frac{(\mu_0+\mu_1\widehat{N}_f)^2}{2\left(\sigma_0^2+2\rho\sigma_0\sigma_1\widehat{N}_f+\sigma_1^2\widehat{N}_f^2\right)}} erf\left[\frac{\mu_0\sigma_1(\rho\sigma_0+\sigma_1\widehat{N}_f)-\mu_1\sigma_0(\sigma_0+\rho\sigma_1\widehat{N}_f)}{\sqrt{2-2\rho^2}\sigma_0\sigma_1\sqrt{\sigma_0^2+2\rho\sigma_0\sigma_1\widehat{N}_f+\sigma_1^2\widehat{N}_f^2}}\right] + \frac{(\mu_0\sigma_1(\rho\sigma_0+\sigma_1\widehat{N}_f)-\mu_1\sigma_0(\sigma_0+\rho\sigma_1\widehat{N}_f))}{\sqrt{2\pi}(\sigma_0^2+2\rho\sigma_0\sigma_1\widehat{N}_f+\sigma_1^2\widehat{N}_f^2)^{3/2}} \quad (8)$$

where:

- $erf(*)$= the error function;
- $\widehat{N}_f$= variable for the predicted failure cycle;
- μ_j= mean estimate of the intercept and slope, denoted with subscript 0 and 1 respectively;
- σ_j= estimated standard deviation of the intercept and slope, denoted with subscript 0 and 1 respectively;
- ρ= correlation coefficient of the intercept and slope of the linear regression.

The PDF can be obtained in real-time to estimate the confidence in the predictions made using the FFM and updated when new data points are obtained while the component is in operation. The results were verified with a Monte-Carlo simulation using synthetic data with random measurement uncertainties characterised by the actual data set from the experiment. The results at $N = 2 \times 10^5$ for both the analytical and 10,000-trial Monte-Carlo simulation is shown in Fig. 9.

3.3. Comparing the inspection and monitoring approach to fatigue life predictions

3.3.1. Statistical comparison between inspection and monitoring

Using the above methods, a comparison between the inspection and monitoring approach to fatigue life predictions can be made. Fig. 10 plots the median life predictions of the inspection and monitoring results. This shows that the predictions made using the monitoring approach converges much more quickly to the actual failure cycle. From $N = 2 \times 10^5$ onwards, approximately half the life of the component, all predictions made using the monitoring approach were within 10% the actual failure cycle. Conversely with the inspection approach, there is no way of adapting or correcting for the actual operation conditions. With each inspection, only the measured crack length can be updated, while no additional information on the loading conditions and material properties can be obtained. Therefore, the predictions made converge slowly to the actual failure time as the end of life of the component

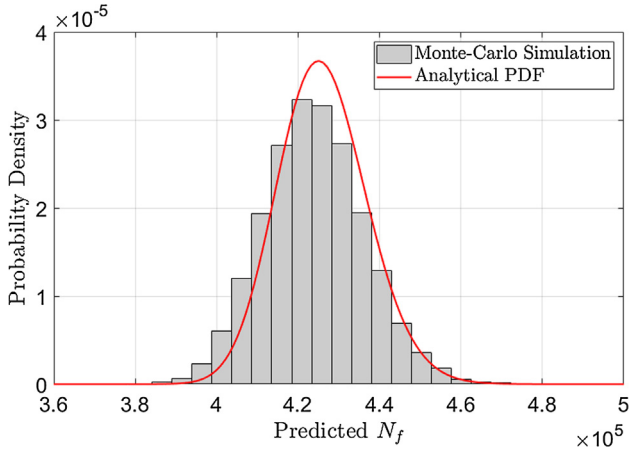


Fig. 9. Plot of the PDF of the predicted failure cycle at $N = 2 \times 10^5$ using the FFM. The histogram represents the results of the Monte-Carlo simulation, the line graph represents the analytical solution.

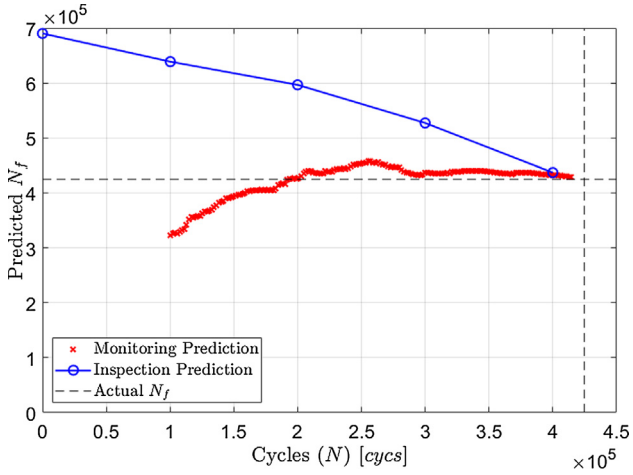


Fig. 10. Plot of the median life predictions against number of loading cycles using the inspection and monitoring approach.

approaches.

Not only are the predictions more accurate with the monitoring approach, the confidence in the predictions made is significantly greater as shown in Fig. 11. Consider the predictions made with both methods at $N = 2 \times 10^5$. Assuming that the target level of confidence in the integrity of the component is 99.7% (3σ), the conservative remnant life prediction made using the inspection and monitoring approach would be $N = 2.8 \times 10^5$ and $N = 3.5 \times 10^5$ respectively. At this point, the estimated remnant useful life of the component would be 0.8×10^5 cycles should the inspection-based approach be used, while with the use of the monitoring-based approach, the component would have an estimated remnant useful life of 1.5×10^5 cycles. Given that an inspection is only performed every 10^5 cycles, the component would fail to meet the required threshold of confidence in integrity before the next inspection. In comparison, due to significantly greater confidence, the conservative predictions made with the monitoring approach are much closer to the actual failure cycle.

While the choices of target confidence and inspection interval here are arbitrary, the study demonstrates how estimations with greater confidence via the monitoring approach make it possible to safely operate the component closer to its actual failure time. These predictions, including the confidence bounds, can be made in real-time while the component is in operation. Thus, the use of monitoring can provide improved awareness of the damage state of the component without the need of inspections, potentially reducing the duration or even the frequency of costly planned outages.

3.3.2. Validity of using the FFM for fatigue life predictions

Despite the life predictions made using the FFM having lower uncertainty, systematic errors resulting in bias in the predictions are also apparent at various stages of the experiment. From Figs. 10 and 11 it is evident that the remnant life is initially underestimated (even falling outside the confidence bounds initially), followed by a near-constant overestimation for the remaining life. These discrepancies are due to a known epistemic error in the method as the fatigue damage passes through different phases of crack growth. Fig. 12(a) shows a typical schematic plot of crack growth rate against stress intensity factor, which is a function of stress, crack length and geometry of a fatigued component. Fig. 12(b) schematically shows how the subsequent plot of inverse crack growth rate against number of cycles would appear. This non-linear relationship between the inverse crack growth rate and number of cycles is the major cause of the systematic error in the predictions made by the FFM. The systematic error in this experiment is however not very significant as the specimen of this test spends most of its fatigue life within the stage II crack growth regime.

The crack growth mechanism is different during initial cycles of fatigue, since the radius of a fatigue crack tip is orders of magnitude smaller than the “crack” that was electrical discharge machined (EDM). Therefore, a fatigue crack would have to “initiate” from the EDM crack. This would have crack growth characteristics that in some ways resemble the stage I crack growth region; remnant life is thus underestimated as the slope of the regression fit of inverse crack growth rate against number of cycles is greater in stage I than in stage II crack growth.

The subsequent overestimation of remnant life can also be explained similarly. During the terminal stages (Stage III) of crack growth, the crack growth rate accelerates and deviates from the linear relationship between crack growth rate and stress intensity factor. This is also reflected in the plot of inverse crack growth rate against number of cycles as demonstrated in Fig. 13, resulting in the component failing earlier than predicted by the FFM. A linear fit is plotted to better illustrate the acceleration in crack growth, which can be seen at around $N = 4 \times 10^5$. However, since this terminal stage of fatigue crack growth is only a very small portion of the overall life of the component, the resulting overestimation is minimal.

It is therefore clear that for the FFM to provide accurate fatigue life predictions, the remnant fatigue life of the component must be dominated by a single damage accumulation mechanism. In the case of this experiment, a majority of the fatigue life of the component is spent at Stage II, Paris law crack growth. Thus, the predictions made in this region were accurate with relatively small systematic error. Such an error also exists with the inspection approach, but since there are such great uncertainties in the predictions, its effect becomes negligible. More advanced empirical crack growth laws such as the Forman equation [25] or the NASGRO equation [26] can be used to better model the crack growth behaviour across multiple stages of fatigue crack growth. However, more input parameters, each with an associated uncertainty, is required for these crack growth laws, resulting in significant uncertainties in the prediction despite the crack growth model being accurate.

3.3.3. Failure criterion of the FFM

As shown earlier in Eq. (5) and (6), it was assumed that the damage accumulation rate at failure is infinite, hence the x-axis intercept of the plot of inverse growth rate against number of cycles is the estimated point of failure. This proves to be a valid assumption as shown in Fig. 13 where the last data point is very close to the x-axis. The validity of this assumption is determined by the requirement that the period of monitoring would need to cover a significant fraction of the crack propagation life of the component such that the range of crack growth rates measured is sufficiently large.

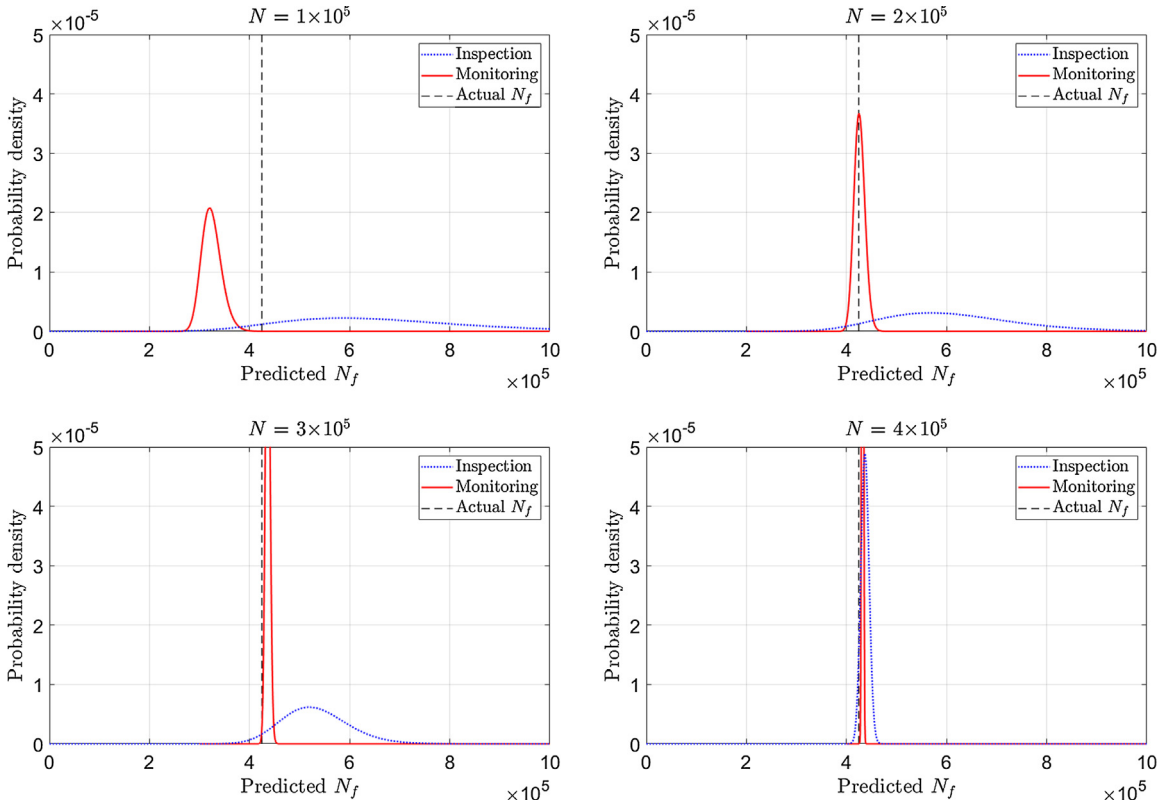


Fig. 11. Plots of the PDFs of the predicted failure cycle at intervals of 10^5 cycles. The dotted graph represents the results from the inspection approach, the solid graph represents the results of the monitoring approach, the dash line indicates when the component actually failed.

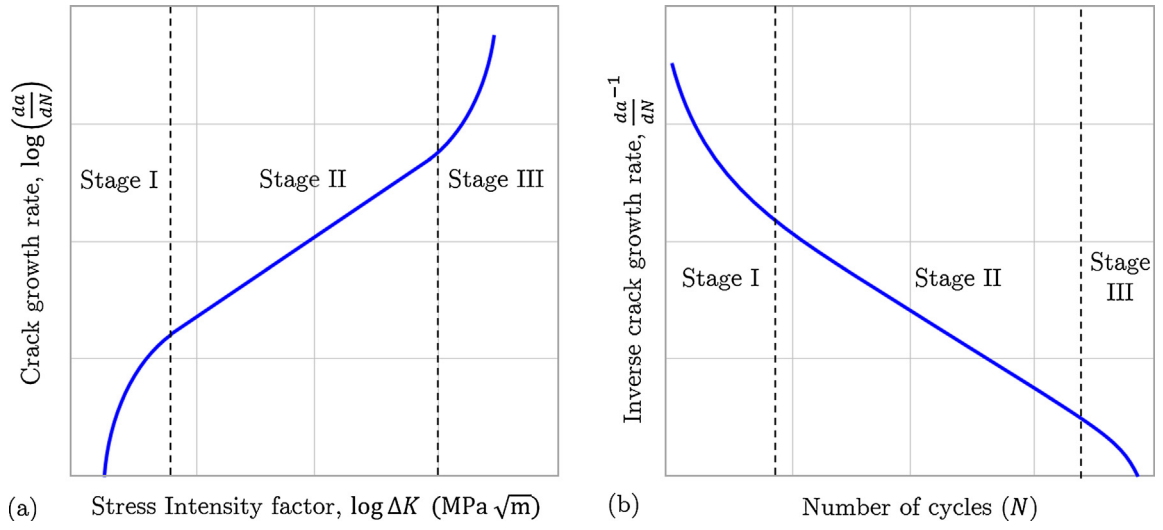


Fig. 12. (a) Illustration of a typical plot of crack growth rate against stress intensity factor, which is a function of stress, crack length and geometry of a fatigued component; (b) resulting plot of inverse crack growth rate against number of cycles.

In industrial engineering applications, there are cases where the failure criterion is instead determined by the ability of the component to withstand a critical load. An example of this would be the ability of an offshore wind turbine structure to withstand loads under extreme weather conditions [27], where failure under nominal loading conditions is no longer the failure criterion for the fitness of service of the component, as assumed with the FFM.

One potential way to accommodate this while using the FFM to perform life predictions is to introduce a finite critical crack growth rate failure criterion. With knowledge of the material properties of the component under its operating conditions as well as the correlation between stress intensity and crack growth rate, a maximum allowable crack growth rate using empirical crack growth laws can be obtained, as schematically demonstrated in Fig. 14. The failure is then estimated to occur at the point where the linear regression of the FFM crosses a specific value of inverse crack growth rate instead of the x-axis intercept. However, this process requires more information on the materials properties and operating conditions, as well as a calibrated conversion between signal change and crack growth rate. This means that the advantage of using the FFM is significantly reduced as more information and thus uncertainties are introduced.

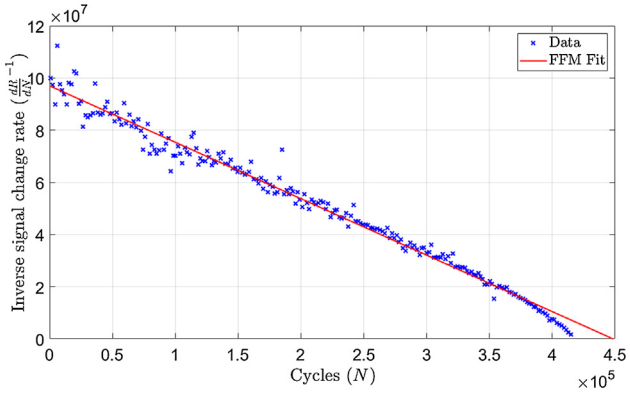


Fig. 13. Plot of inverse signal change rate against number of cycles from the fatigue experiment, highlighting how the change in crack growth rate deviates from the linear relation at terminal stages of fatigue crack growth.

4. Failure forecast method for non-constant amplitude loading

Real-life engineering components are often subjected to varying loading conditions that cannot be simplified to a constant amplitude fatigue problem. It is therefore important to understand the capabilities of the FFM for fatigue damage monitoring under non-constant amplitude loading. Three cases of loading are considered and evaluated via experiments in this section; a step change in loading condition, isolated overloads, and variable amplitude loading.

4.1. Step change in loading condition

The first case of non-constant amplitude loading considered is a step change in loading conditions. This might occur, for example, when a defect is found in a power station component, where it is common to derate the unit to reduce the stresses and so extend the component life. A method of compensating for a change in loading conditions while using the FFM is proposed.

Voight briefly outlined an expanded version of the integrated form of his equation to account for variable stresses at failure [23]. For $\alpha > 1$,

$$\frac{d\Omega}{dt} = \left(A\left(\alpha-1\right)\left(t_f - t\right) + \left(\frac{d\Omega}{dt}\Big|_f \left(\frac{\sigma}{\sigma'}\right)^n\right)^{1-\alpha}\right)^{\frac{1}{1-\alpha}} \tag{9}$$

where σ' is some reference stress, σ is the estimated stress level at failure, which in the case of a step change in loading condition would be the new load, and n is an empirical constant.

It is proposed that the above equation can be expressed in a more useful form by introducing the variables,

$$t_{eq} = t \times \left(\frac{\sigma}{\sigma'}\right)^{n(\alpha-1)}, \qquad t_{eq,f} = t_f \times \left(\frac{\sigma}{\sigma'}\right)^{n(\alpha-1)} \tag{10}$$

Substituting Eq. (10) into Eq. (9), rearranging and assuming infinite growth rate at failure,

$$\frac{d\Omega}{dt_{eq}} = \left(A\left(\alpha-1\right)\left(t_{eq,f} - t_{eq}\right)\left(\frac{\sigma}{\sigma'}\right)^{n(\alpha-1)(\alpha-2)}\right)^{\frac{1}{1-\alpha}} \tag{11}$$

Putting this in context of fatigue crack propagation,

$$\frac{da}{dN_{eq}} = \left(A\left(\alpha-1\right)\left(N_{eq,f} - N_{eq}\right)\left(\frac{\Delta\sigma}{\Delta\sigma'}\right)^{n(\alpha-1)(\alpha-2)}\right)^{\frac{1}{1-\alpha}} \tag{12}$$

where,

$$N_{eq} = N \times \left(\frac{\Delta\sigma}{\Delta\sigma'}\right)^{n(\alpha-1)}, \qquad N_{eq,f} = N_f \times \left(\frac{\Delta\sigma}{\Delta\sigma'}\right)^{n(\alpha-1)} \tag{13}$$

This definition of equivalent cycles is similar to Basquin's exponential law for fatigue, which states that there is a power law relationship between the fatigue life of a component and the loading amplitude the component experiences [28]. What is shown here is that a similar relation can be used in crack growth monitoring and FFM to compensate for the effect of change in loading. It is also observed that the empirical constant n should equate to the Paris' exponent m. Assuming linear-elastic fracture mechanics, the Paris law is,

$$\frac{da}{dN} = C(\Delta K)^m = C(Y(a)\Delta\sigma\sqrt{a})^m \tag{14}$$

It can be seen that the crack growth rate is proportional to the stress range raised to the power of m, hence it would be reasonable to assume that the two empirical constants are equal.

As mentioned earlier, it is reasonable to assume $\alpha = 2$. Therefore, Eq. (12) simplifies to,

$$\left(\frac{da}{dN_{eq}}\right)^{-1} = A\left(N_{eq,f} - N_{eq}\right) \tag{15}$$

This is identical to Eq. (6), that was used for the FFM analysis in previous sections, but with equivalent cycles replacing the actual cycles of loading. This shows that by introducing the definition of equivalent

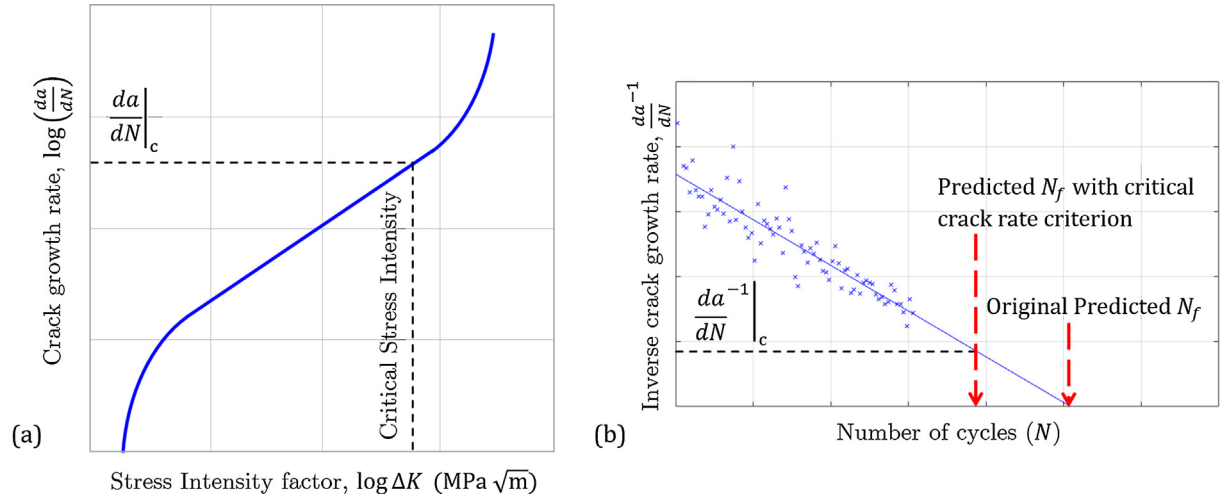


Fig. 14. Schematic demonstration of how a finite critical crack growth rate can be introduced in the FFM. (a) illustration of how a critical crack growth rate can be defined from the plot of crack growth rate against stress intensity factor; (b) graph demonstrating how this can be implemented while using the FFM.

Table 3
Geometry and loading parameters of the fatigue test with change in loading conditions in accordance to ASTM 647-15e1 [20] as shown in Fig. 3.

Parameter	Value
W (mm)	80
B (mm)	20
a (mm)	16
Maximum load, P_{max} (kN)	35 kN for the first 4×10^4 cycles, then 28 kN until failure
Load ratio, R	0.1

cycles N_{eq}, continuity of relation between the crack growth rate and number of cycles can be retained despite changes in loading amplitudes. Thus, the same method as discussed in Section 3 can be used to perform fatigue life predictions while taking into account the change in operating conditions, given that the relative change in loading, $\frac{\Delta\sigma}{\Delta\sigma'}$, and the Paris' exponent m are both known.

To validate the equivalent cycles method for compensating step changes in loading conditions, a fatigue experiment using a CT specimen made of S275 steel with parameters shown in Table 3 was conducted while crack growth was monitored using the front-face compliance method using clip gauges. The experiment simulates the case where it is proposed that a defective engineering component is to be operated at derated conditions to limit the crack growth rate and it is necessary to predict the remnant life given the new loading. In this example, the maximum load is reduced by 20% while the load ratio remains constant. The experiment compares the accuracy and confidence in the predictions made in the following two cases. The first case is where no monitoring system was used, so an inspection to measure the crack length is conducted immediately prior to the derating to estimate the remnant life of the component. The second case is where a monitoring system was installed on the component long before the derating, hence the FFM with the equivalent cycles method can be used to estimate the remnant life of the component using previously-collected data.

A plot of crack length against the number of cycles of the experiment is shown in Fig. 15(a). The data points represented as crosses and circles are data collected before and after the change in loading respectively; the data collected prior to the change in loading is used for the FFM prediction. Fig. 15(c) and (d) show the inverse crack growth rate against number of cycles and equivalent inverse crack growth rate against equivalent number of cycles respectively. The use of the equivalent cycles method in Fig. 15 restores the continuity of the plot of inverse crack growth rate against cycles, allowing for the use of FFM for fatigue failure analysis where the loading is not at constant amplitude. The FFM regression fits shown on the graphs were obtained using data collected from the first 4×10^4 cycles before the reduction in loading. Note that inverse crack growth rate is used only because calibrated measurements of crack length were readily accessible with this monitoring system. Should a different monitoring system that satistifes the requirements detailed in [15] is used, conversion from signal change to growth rate is not necessary.

To quantify the accuracy and confidence in the use of the FFM for remnant life predictions with load changes using the equivalent cycles method, a statistical analysis similar to that discussed previously was performed. In addition to the uncertainties in damage growth rate measurement, the uncertainties in the loading conditions and Paris exponent now have to be considered. The relative change in loading is assumed to have a mean of 20% and a standard error of 2%. The uncertainty in the Paris exponent is not considered in BS7910. Therefore in this analysis, the Paris exponent is assumed to have a mean of $m = 2.88$ and a coefficient of variation, $COV = 0.0582$. The mean value is from the BS7910, while the COV was obtained from the statistical analysis by Gobbato [10] of the Virkler fatigue test data [6]. For comparison, a statistical analysis was also performed for the periodic inspection case with the same uncertainties shown earlier in Table 2.

Fig. 16 shows the results of the analysis. The dotted lines show the probability density functions of the remnant life estimation assuming the original loading conditions; of course these predictions underestimate the failure time as the true remnant life was extended by the derating. The corrected remnant life estimates based on the assumed change in load is shown in Fig. 16 with solid lines. As with the constant load results of Fig. 11, the uncertainty in the life prediction made with the FFM is lower than that from the inspection based approach. However, the improvement is not as large as the constant amplitude loading results. In order to account for the change in loading, the FFM now relies on the relative change in loading conditions and the Paris exponent, each with associated uncertainty, which translates to less confident predictions. Overall, it is demonstrated that by using this equivalent cycle method for FFM, more confident predictions in remnant life can be made prior to changes in operating conditions than conducting an inspection immediately before the change.

It can be seen from Fig. 16 that the FFM underestimates the remnant life after the change in loading. This underestimation is caused by crack growth retardation as a result of local plastic deformation at the crack tip, similar to the effect of an overload [29]. Fig. 15(c) shows a sudden increase in inverse crack growth rate (ie. decrease in crack growth rate) for an appreciable period after the load decreases. The initial cycles at high load create a comparatively larger plastic zone in front of the crack tip, which the initial cycles of the low load have to propagate through. This results in a decrease in crack growth rate and subsequently extends the life of the component beyond what would be predicted before derating, effectively shifting the actual failure time into the future, thus the discrepancy. For the inspection approach, empirical compensations have been developed to account for the effect [30,31], but again more input parameters with uncertainties would have to be introduced, resulting in greater uncertainties in the predictions made.

The retardation following a derating illustrates that it is important to understand how the use of the FFM is affected by the effect of such loading interaction effects, namely crack growth behaviour that is dependent on load history, This is a key step to implementing fatigue monitoring in industrial applications where loading is often non-constant.

4.2. Isolated overloads

To illustrate and evaluate the effect of isolated overloads on predictions made using the FFM, an experiment identical to the one detailed in Section 2 is conducted, except that two single-cycle overloads with maximum loads 40% and 60% greater than a normal cycle were introduced during the tests at around $N = 2 \times 10^5$ and 3×10^5 respectively. Fig. 17 plots the (a) crack length and (b) inverse signal change rate against number of cycles. Initial cycles after the overload are affected by the plastic zone generated by the overload, and then resumes as normal as the crack tip exits the overload plastic zone. As a result, an overload would effectively translate the plot of inverse signal change rate against number of cycles to the right. From Fig. 17, it is evident that starting from approximately 5×10^4 cycles after an overload, the linear relation between inverse damage accumulation rate and number of cycles is restored and subsequent data can be used to perform life predictions using the standard FFM.

In industrial applications, this means that once the component has operated for a period of time after the overload, it is always possible to restart the FFM prediction with only the data collected afterwards. It is also believed to be possible to use the gradient of the initial FFM fitting as a prior estimation of the slope for the FFM fitting of the data collected after the overload. Moreover, monitoring data can clearly indicate when an overload has occurred, and so is beneficial in understanding the damage state of the component.

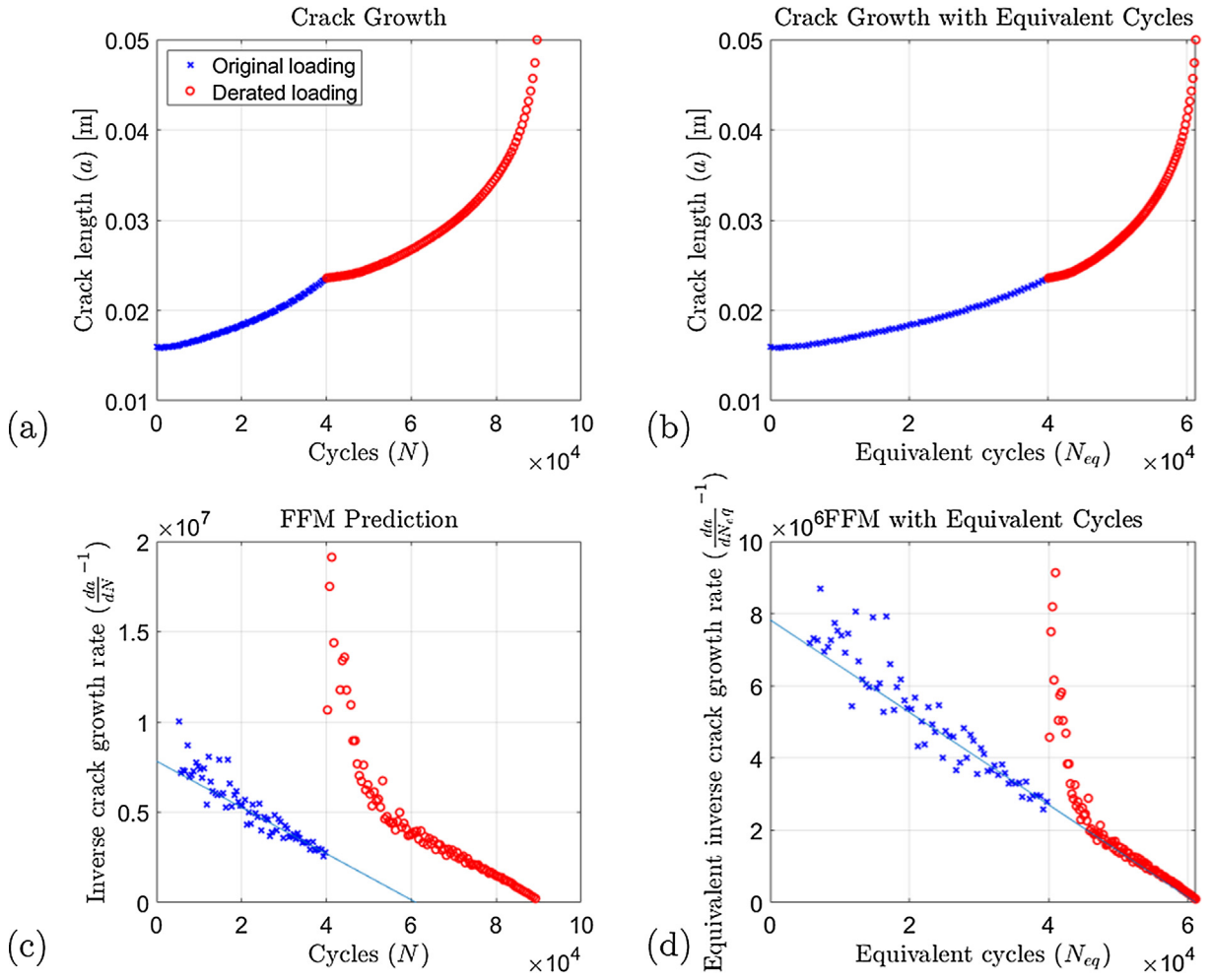


Fig. 15. Plot of (a) crack length against number of cycles; (b) crack length against number of equivalent cycles; (c) inverse crack growth rate against number of cycles; (d) equivalent inverse crack growth rate against number of equivalent cycles for the fatigue experiment with a change in loading conditions. Crosses and circles represent data points prior to and after the change in loading conditions.

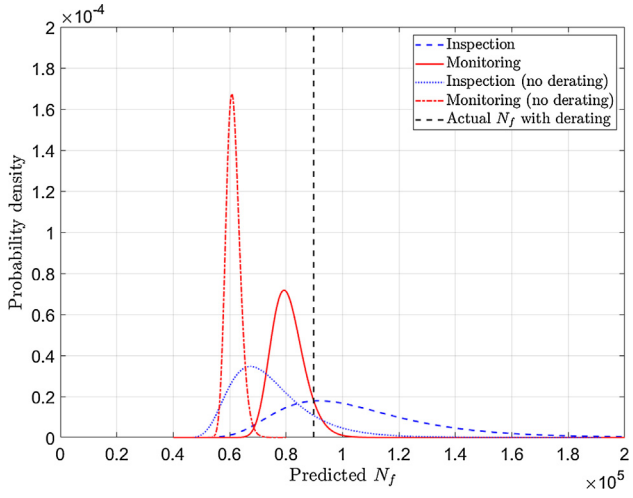


Fig. 16. Plots of the fitted PDF for the predicted failure prior to the change in loading. Both the predictions made with and without considering the change in loading are plotted. The vertical dash line represents when the component actually failed.

4.3. Variable amplitude loading

Other than isolated overloads, there are also cases where overloads and underloads occur periodically during the life cycle of a component. These components may be subjected to variable amplitude loadings that can be described by a probability distribution [32]. The combination of high and low loads result in retardation and acceleration effects as the sequence of these loadings affect the state of the local stress-strain field ahead of the crack tip [33].

In order to investigate these effects, a fatigue experiment with variable amplitude loading was conducted. The specimen geometry was as described in Table 1, but with initial crack length of 25.5 mm. The component was loaded at a constant mean load of 4.125 kN and load range following a log-normal distribution where $\mu = 1.90$ and $\sigma = 0.100$, which translates to a mean load range of 6.75 kN and a coefficient of variation of 0.1. Fig. 18 shows (a) a small sample of the loading and (b) a plot of the distribution of load ranges; the results are shown in Fig. 19.

It can be seen that the linear relationship between inverse crack growth rate and number of cycles as postulated by the FFM still holds with variable amplitude loading that is statistically stationary. In cases where the loading of a component remains statistically stationary and monitoring data is collected over a significant period of time, predictions made using the FFM would still be valid. While individual rate data points may be skewed by load interaction effects, it is believed that with sufficient data points covering a long enough period of time, the

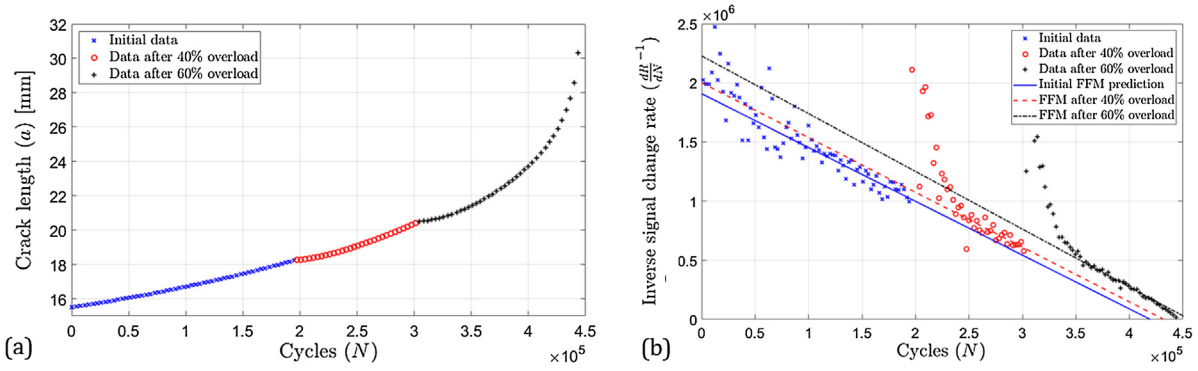


Fig. 17. Plot of crack length (a) and inverse signal change rate (b) against number of cycles for the overload test.

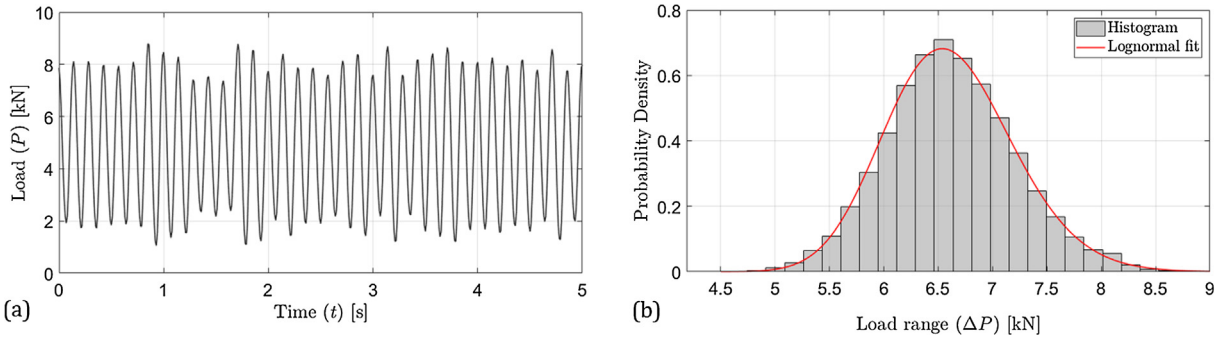


Fig. 18. Plot of (a) a small sample section of the loading and (b) distribution of load ranges measured from the experiment.

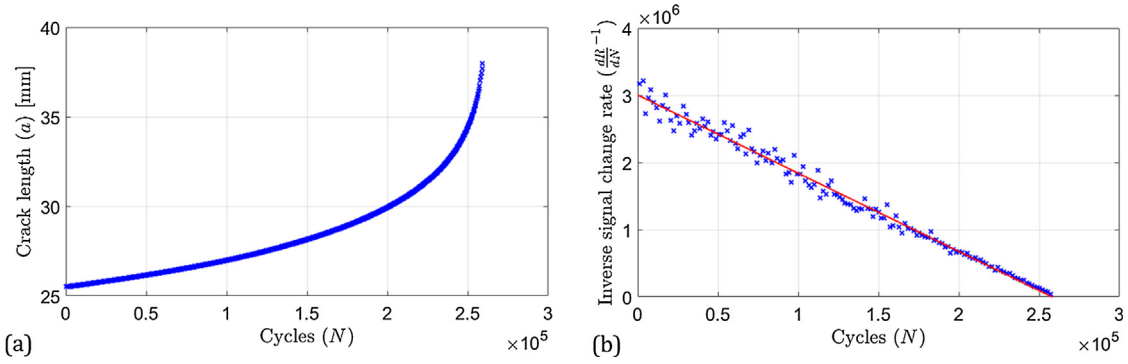


Fig. 19. Plot of (a) crack length and (b) inverse signal change rate against number of cycles for the random loading test.

overall prediction made by the FFM would remain accurate. This conceptually demonstrates how FFM can be capable of performing remnant life predictions with variable amplitude loading. However, it is believed that more research should be conducted with a wider range of distributions, particularly those of relevance in industrial applications, and loadings of greater variability should be tested to better understand and quantify the capabilities and limitations of using the FFM under variable amplitude loading conditions.

5. Conclusions

The accuracy and uncertainty in remnant life predictions made using crack size measurements from conventional periodic inspection and damage growth rate based estimates from permanently installed monitoring have been compared on data from a fatigue test instrumented with a potential drop measurement system. The remnant life estimates obtained from the permanently installed monitoring system using the Failure Forecast Method provided more accurate remnant life predictions with much greater confidence than estimates from the conventional approach using crack length measurements and Paris Law. The smaller uncertainty in the estimates using the Failure Forecast Method is largely due to it being based simply on the rate of increase of the damage-related signal with no requirement for knowledge of the load or material constants.

The use of the Failure Forecast Method under non-constant amplitude loading was also evaluated. A modified version of the Failure Forecast Method can be used to accommodate step changes in loading, but the load change must be measured and the relationship between load and crack growth rate must be known, so increasing the data requirements and the resulting uncertainty in the estimates. The effect of load interaction on the use of the Failure Forecast Method was also discussed using experimental data of a fatigue test with isolated overloads and random variable amplitude loading. Experimental results demonstrate that the Failure Forecast Method remains valid for random variable amplitude loading that is statistically stationary, while isolated overloads can be easily detected and accounted for by restarting the process.

The basic Failure Forecast Method assumes infinite damage growth rate at failure. The fitness-for-service criterion is sometimes the ability of the structure to withstand an extreme load, rather than integrity

under normal loading. It has been discussed how the Failure Forecast Method can be adapted to deal with this case, but again at a cost of more information on material properties and loading conditions being required.

The study has shown that the frequent data obtained from permanently installed monitoring systems provides new opportunities in remnant life estimates and potentially opens the way to increasing the intervals between outages and reducing design conservatism.

Acknowledgements

This work was supported by the UK Engineering and Physical Sciences Research Council via the UK Research Centre in NDE, grant EP/L022125/1.

References

[1] Suresh S. Fatigue of materials (Cambridge solid state science series). 2nd ed. Cambridge University Press; 1998.
[2] Engesvik KM, Moan T. Probabilistic analysis of the uncertainty in the fatigue capacity of welded joints. Eng Fract Mech 1983;18(4):743–62.
[3] Stutzmann J, Ziegler L, Muskulus M. Fatigue crack detection for lifetime extension of monopile-based offshore wind turbines. Energy Proc 2017;137:143–51.
[4] Cheng J, Potter JN, Croxford AJ, Drinkwater BW. Monitoring fatigue crack growth using nonlinear ultrasonic phased array imaging. Smart Mater Struct 2017;26(5):055006.
[5] Ahmed S, Schumacher T, Thostenson ET, McConnell J. Simultaneous life extension and crack monitoring of fatigue-damaged steel members using multifunctional carbon nanotube based composites. In: Tribikram Kundu, editor. Health monitoring of structural and biological systems 2017. SPIE; April 2017.
[6] Virkler DA, Hillberry BM, Goel PK. The statistical nature of fatigue crack propagation. Technical report AFFDL-TR-78-43, Air Force Flight Dynamics Laboratory; 1979.
[7] Ortiz K, Kiremidjian AS. Stochastic modeling of fatigue crack growth. Eng Fract Mech 1988;29(3):317–34.
[8] Guide to methods for assessing the acceptability of flaws in metallic structures. BS7910:2013 + A1:2015. The British Standards Institution; 2015.
[9] Probabilistic methods for planning of inspection for fatigue cracks in offshore structures, DNVGL-RP-C210, DNV GL; 2015.
[10] Gobbato M, Conte JP, Kosmatka JB. Statistical performance assessment of an NDE-based SHM-DP methodology for the remaining fatigue life prediction of monitored structural components and systems. Proc IEEE 2016;104(8):1575–88.
[11] Rudolph J, Bergholz S. The AREVA integrated and sustainable concept of fatigue design, monitoring and re-assessment. In: Codes and standards, vol. 1. ASME; 2008.
[12] Carden EP, Fanning P. Vibration based condition monitoring: a review. Struct Health Monitor: Int J 2004;3(4):355–77.
[13] Bo Z, Yanan Z, Changzheng C. Acoustic emission detection of fatigue cracks in wind turbine blades based on blind deconvolution separation. Fatigue Fract Eng Mater Struct 2016;40(6):959–70.
[14] Jiao S, Cheng L, Li X, Li P, Ding H. Monitoring fatigue cracks of a metal structure using an eddy current sensor. EURASIP J Wirel Commun Network 2016;2016(1).
[15] Corcoran J. Rate-based structural health monitoring using permanently installed sensors. In: Proceedings of the Royal Society of London A: mathematical, physical and engineering sciences, vol. 473 (2205); 2017.
[16] Voight B. A relation to describe rate-dependent material failure. Science 1989;243(4888):200–3.
[17] Paris P, Erdogan F. A critical analysis of crack propagation laws. J Basic Eng 1963;85(4):528–33.
[18] Garrido OC, Shawish SE, Cizelj L. Crack growth assessment in pipes under turbulent fluid ixing using an improved spectral loading approach and linear elastic fracture mechanics. In: 25th international conference nuclear energy for New Europe. NENE; 2016.
[19] Zentuti NA, Booker JD, Bradford RAW, Truman CE. A review of probabilistic techniques: towards developing a probabilistic lifetime methodology in the creep regime. Mater High Temp 2017;34(5–6):333–41.
[20] Standard test method for measurement of fatigue crack growth rates. ASTM E647-15. ASTM International; 2016.
[21] Information for the procurement and conduct of ndt, part 4: Ultrasonic sizing errors and their implication for defect assessment. Health and Safety Executive; 2008.
[22] Moles M, Wesley L, Sinclair T. Accurate defect sizing using phased array and signal processing. In: Developments in ultrasonics inspection II. JRC NDE; 2009.
[23] Voight B. A method for prediction of volcanic eruptions. Nature 1988;332:125–30.
[24] Todd MD, Leung M, Corcoran J. A probability density function for uncertainty quantification in the failure forecast method. In: 9th European workshop on structural health monitoring. BINDT; July 2018.
[25] Forman RG, Kearney VE, Engle RM. Numerical analysis of crack propagation in cyclic-loaded structures. J Basic Eng 1967;89(3):459.
[26] NASGRO Consortium. Fatigue crack growth computer program NASGRO®version 3. 0. user manual, jsc-22267b. NASA Technical report; 2001.
[27] Yeter B, Garbatov Y, Soares CG. Reliability of offshore wind turbine support structures subjected to extreme wave-induced loads and defects. In: Structures, safety and reliability, vol. 3. ASME; June 2016.
[28] Basquin HO. The exponential law of endurance tests. In: American society for testing and materials proceedings, vol. 10; 1910. p. 625–30.
[29] Ray A, Patankar R. Fatigue crack growth under variable-amplitude loading: Part i - Model formulation in state-space setting. Appl Math Model 2001;25(11):979–94.
[30] Wheeler OE. Spectrum loading and crack growth. J Basic Eng 1972;94(1):181.
[31] Willenborg J, Engle RM, Wood HA. A crack growth retardation model using an effective stress concept. Technical report AFFDL-TM-71-1-FBR. Air Force Flight Dynamics Laboratory; 1971.
[32] Ziegler L, Schafhirt S, Scheu M, Muskulus M. Effect of load sequence and weather seasonality on fatigue crack growth for monopile-based offshore wind turbines. Energy Proc 2016;94:115–23.
[33] Mills WJ, Hertzberg RW. Load interaction effects on fatigue crack propagation in 2024-t3 aluminum alloy. Eng Fract Mech 1976;8(4):657–67.